AIAA 81-4262

Potential Flow about Bodies of Revolution with Mixed Boundary Conditions—Cross Flow

J.V. Rattayya,* J.A. Brosseau,† and M.A. Chisholm‡
Lockheed Missiles & Space Company, Inc., Sunnyvale, Calif.

The computation of hydrodynamic forces and moments acting on an axisymmetric body with a trailing cavity in planar motion is formulated, taking into account the lateral deflection of the cavity surface. The basic premise employed is that, for small cavity deflections, the potential flow associated with the nonaxisymmetric body-cavity configuration can be calculated by assuming the undeflected body-cavity configuration and assigning deflection-dependent source distributions over that surface such that the appropriate mixed boundary conditions are satisfied. The potential flow solutions associated with rigid body translation and rotation are then solved separately using an iteration technique similar to the one used for the axial flow case. The pressure distribution on the body in motion is then computed and compared with measured pressure data in simulated free flights. The computed hydrodynamic coefficients are also presented as a function of Froude and cavitation numbers.

Nomenclature

A_b = body base (reference) area
C_p = pressure coefficient = $p/\frac{1}{2}\rho U_\infty^2$
$C_{x\dot{u}}, C_{xuu}$ = hydrodynamic axial force coefficients associated with axial acceleration and velocity
$C_{N\alpha}, C_{Nq}$ = static hydrodynamic normal force coefficients
$C_{M\alpha}, C_{Mq}$ = static pitch moment coefficients
$C_{N\dot{w}}, C_{N\dot{q}}$ = inertial hydrodynamic normal force coefficients
$C_{M\dot{w}}, C_{M\dot{q}}$ = inertial hydrodynamic pitch moment coefficients
d = body base diameter
F = Froude number = $U_\infty/\sqrt{gL_B}$
F_x, F_z = force components acting on the body in x and z directions, respectively
f_c, f_u, f_w, f_q = derivatives of velocity potentials ϕ_c, ϕ_u, ϕ_w, and ϕ_q along the meridian direction
g = gravitational acceleration
g_c, g_u, g_w, g_q = derivatives of velocity potentials ϕ_c, ϕ_u, ϕ_w, and ϕ_q in the direction normal to the body surface
L = body length
l_B = distance to the body base from the origin of the body-fixed coordinate system (see Fig. 1)
l_n = distance to the body nose from the origin of the body-fixed coordinate system (see Fig. 1)
M_y = pitching moment
n = number of segments
N = normal derivative
p = pressure
q = pitch velocity
q_s, q_θ = fluid velocity components in S and θ directions relative to the body
R = body radius
r_{PQ} = linear distance between points P and Q
S = distance along meridian
s = surface area
u, w = body velocity components along axial and normal directions
U_∞ = freestream velocity
x, y, z = body-fixed rectangular coordinates
x, r, θ = body-fixed polar coordinates
V_N, V_S, V_θ = body velocity components in normal, meridional, and circumferential directions respectively on its surface
V_T = fluid velocity relative to the body in the meridional direction for unit axial motion of the body
Z_c = cavity displacement distance in z-direction
ΔC_p = difference in pressure coefficient across the body
Φ = velocity potential
ϕ_u, ϕ_w, ϕ_q = perturbation velocity potentials associated with axial, normal, and rotational body motions
δ_c = cavity deflection angle
α = angle of attack = $\tan^{-1} w/u$
σ = source strength on the body surface
β = body slope
ρ = fluid density

Subscripts

B = body
b = base
c = cavity or cross flow

Received Aug. 1, 1979; revision received July 6, 1981.

*Staff Engineer. Member AIAA.
†Research Specialist.
‡Research Specialist.

I. Introduction

THE hydrodynamic forces and moments acting on an axisymmetric body with attached cavities undergoing planar motion depend not only on the cavity configuration, but also on its deflection relative to the body axis. As long as the axial motion is predominant in comparison with lateral translation and rotation, the deflection is expected to be small. When cavity deflection is neglected, the cavity can be treated as the rigid extension of the body, and the analysis of Ref. 1 can be used to compute the hydrodynamic force and moment coefficients. In this scheme, the body is assumed rigid, and the Neumann problem is solved separately for axial flow, uniform cross flow, and nonuniform cross flow. These solutions are then combined to compute pressure and, hence, the force and moment acting on the moving body.

Recently, Struck[2] has studied the mixed boundary value problem associated with an axisymmetric body and the freestream line that separates the body wake from the potential flow. Assuming the body is at small angles of attack, Struck developed an appropriate technique for taking into account the deflection of the wake while computing the forces and moments acting on the body. In this procedure, the shape of the wake as obtained in the axial flow case was assumed for the angle of attack case, but the wake was shifted to a position where the local normal force on it is zero. Using a series devel-

opment and linearization, the potential of the asymmetric wake problem was reduced to that of a straight one, with continuously varying angle of attack on the wake portion. The procedure is equally applicable to bent cavities trailing axisymmetric bodies in planar motion.

The principal advantage of Struck's procedure is that an asymmetric Neumann problem is reduced to that of an axisymmetric one with somewhat modified source strength distribution. From this point of view, the basic force and moment coefficient integral relations applicable to axisymmetric bodies are still valid for asymmetric cavity problems. The integrands involve the unit perturbation potentials and the corresponding velocity components. These perturbation potentials and the corresponding velocity components, however, must be computed so as to account for this asymmetric cavity deflection. Such a computation forms the basis of this paper. Thus, this work represents an extension of Struck's work for small angles of attack to that of bodies in planar motion involving translation as well as rotation. Furthermore, the effects of a gravitational field, which are omitted in Struck's work, will be included here.

For the sake of completeness and ease of reference, the planar motion potential flow problem is briefly presented in Appendix A. The appropriate integral expressions for the hydrodynamic force and moment coefficients will be listed there. Assuming the body-cavity configuration derived in the axial-flow companion to this paper,[3] the cavity deformation, velocity potential, and induced velocities associated with unit uniform cross flow and unit rotation will be solved in Sec. II. The computed force and moment results will be discussed in Sec. IV.

II. Cross Flow Solution with Mixed Boundary Conditions

The force and moment acting on an axisymmetric body in planar motion can be computed, provided the unit velocity potentials ϕ_u, ϕ_w, ϕ_q and their derivatives are known on the surface of the body along the meridian $\theta = 0$ (see Appendix A). The computation of ϕ_u and the cavity configuration with mixed-boundary conditions has been discussed in Ref. 3. In the presence of cross flow, the cavity deflects and we assume such a deflection is small enough to permit some simplifications to the mathematical problem as presented in Appendix B. Such an approximation will allow direct extension of the methodology developed for the numerical computation of cross flow velocity potential on axisymmetric bodies with rigid boundary conditions (Ref. 2) to computing velocity potential with mixed-boundary conditions. The computation of the actual deflection of the cavity should result from such a scheme.

In the case of the rigid body problem, (Ref. 2), the cross flow velocity potential can be computed by ignoring the relative magnitude of the cross flow with respect to the axial flow component. In the mixed-boundary value problem, however, the cavity configuration is affected by axial velocity and the cavity deflection by both axial and cross flow velocity components. For this reason, the cross flow velocity cannot be assigned independent of the axial component. Rather, it must be assigned a fraction of the axial flow component and the corresponding potential determined. The desired cross flow velocity potentials ϕ_w and ϕ_q are obtained by scaling up these computed values. To obtain the limits of applicability of these results, let us consider the body in planar motion (Fig. 1). The cross flow velocity for this motion corresponds to the negative of the missile velocity in z-direction along its axis

$$w_c(x) = -w + qx$$

Normalizing this with axial flow velocity component u, one gets

$$\frac{w_c(x)}{u} = -\frac{w}{u} + \left(\frac{qL}{u}\right)\frac{x}{L}$$

where L is the body length. Note the right-hand side of the above expression is equal to the tangent of the local angle of attack of the missile. The fact that this should be small implies that both $w/u \ll 1$ and $qL/u \ll 1$ must be satisfied for this theory to be valid.

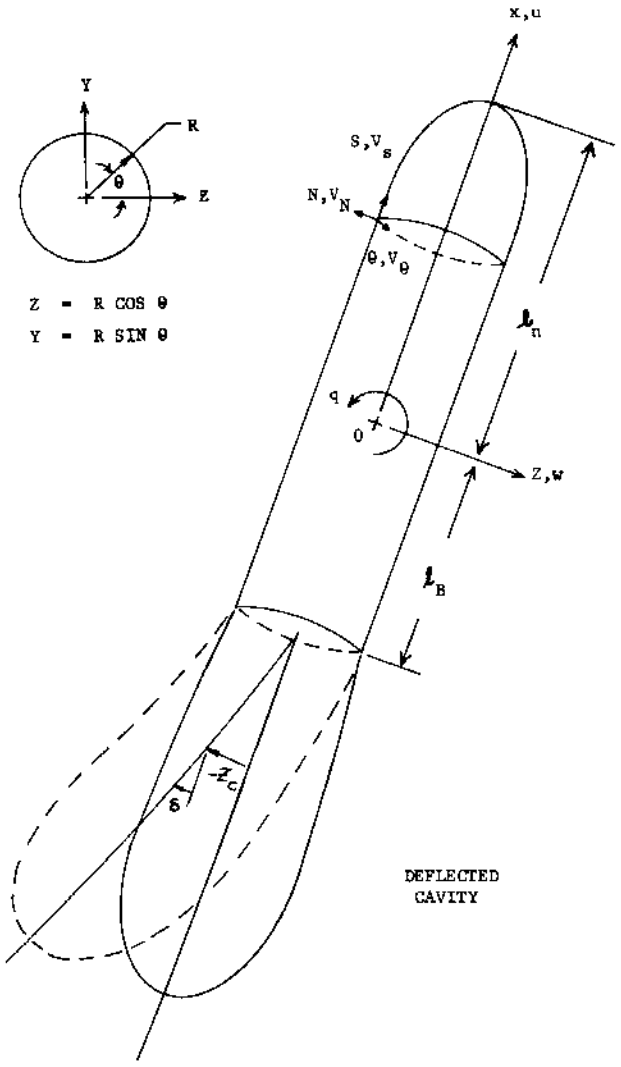

Fig. 1 Body coordinate system and notation.

A. Cross Flow Solution at Small Angle of Attack (Uniform Cross Flow)

1. Problem Formulation

An axisymmetric body with an attached base cavity of known geometry is undergoing translations both in axial and transverse directions. As long as axial motion is dominant, the angle of attack of the body remains small. The cavity, being a free surface, cannot withstand the normal force induced by the cross flow and hence deflects. For small angles of attack the cavity deflection is also small, but varies along its length. If the angular deflection of the cavity is $\delta(x)$, the linear deflection of the centerline, $Z_c(x)$, is given by

$$Z_c(x) = -\int_{-l_B}^{x} \delta(x)\,dx \qquad (1)$$

If the body makes an angle of attack α_B, the local angle of attack $\alpha_c(x)$ on the cavity is given by

$$\alpha_c(x) = \alpha_B - \delta(x) \tag{2}$$

If the body is moving with unit velocity, the cross flow velocity on the body cavity system acting in the z-direction is given by

$$\begin{aligned} w_c(x) &= -\alpha_B \qquad -l_B \le x \le l_n \\ &= -\alpha_c(x) \qquad x < -l_B \end{aligned} \tag{3}$$

For axisymmetric bodies, the total cross flow potential $\Phi_c(x,r,\theta)$ can be expressed as a summation of on-set flow velocity potential $-w_c(x)z$, and the disturbance velocity potential $\phi_c(x,r,\theta)$

$$\Phi_c(x,r,\theta) = -w_c(x)z + \phi_c(x,r,\theta) \tag{4}$$

The perturbation potential ϕ_c can be generated by assigning a singularity distribution $\sigma(S,\theta)$ on the body surface. For small angles of attack, it is reasonable to assume

$$\sigma(S,\theta) = \sigma(S)\cos\theta \qquad \phi_c(x,r,\theta) = \phi_c(x,r)\cos\theta \tag{5}$$

The appropriate integral relation for the potential $\phi_c^{(P)}(x^*,r^*,\theta^*)$ at the field point $P(x^*,r^*,\theta^*)$ is

$$\begin{aligned} \phi_c^{(P)}(x^*,r^*,\theta^*) &= \phi_c^{(P)}(x^*,r^*)\cos\theta^* \\ &= \iint_S \frac{[\sigma_c(S)\cos\theta]^{(Q)}}{r_{PQ}}\, ds^{(Q)} \end{aligned} \tag{6}$$

In this relation, r_{PQ} represents the distance between the field point P and the source point $Q(x,R(x),\theta)$ on the body surface

$$r_{PQ}^2 = (x^*-x)^2 + (y^*-y)^2 + (z^*-z)^2 \tag{7}$$

where

$$y^* = r^*\sin\theta^* \qquad z^* = r^*\cos\theta^*$$

$$y = R\sin\theta \qquad z = R\cos\theta$$

Here, the source strength $\sigma_c(S)$ is an unknown quantity. It is such as to satisfy the boundary condition

$$\partial\Phi_c/\partial N = 0 \tag{8}$$

on the body and cavity surface. Here N indicates the normal derivative.

An additional boundary condition to be satisfied on the cavity arises from the requirement that the normal force acting on the cavity in the z-direction is zero. From the relations (A10) and (A11), it can be inferred that the appropriate relation to be satisfied in the absence of body acceleration is

$$f_c + w_c\sin\beta = 0 \qquad \text{or} \qquad -\partial\phi_c/\partial S + w_c\sin\beta\cos\theta = 0 \tag{9}$$

Note the velocity potential ϕ_c depends on the cavity deflection $\delta(x)$, which is unknown. Thus, the basic mathematical problem herein is to find $\sigma_c(S)$ and $\delta(x)$ such that relations (8) and (9) are satisfied simultaneously.

To construct the solution, one chooses the field point P on the surface of the body itself. The boundary condition, Eq. (8), at point P can be expressed in the form

$$\begin{aligned} &-2\pi\sigma_c(S^*)\cos\theta^* - \sin\beta^* \iint_S \sigma_c(S^{(Q)})\frac{\partial}{\partial x}\left(\frac{1}{r_{PQ}}\right)\cos\theta^{(Q)}\, ds^{(Q)} \\ &+ \cos\beta^* \iint_S \sigma_c(S^{(Q)})\frac{\partial}{\partial R}\left(\frac{1}{r_{PQ}}\right)\cos\theta^{(Q)}\, ds^{(Q)} \\ &+ w_c(x^*)\cos\beta^*\cos\theta^* = 0 \end{aligned} \tag{10}$$

Similarly the boundary condition, Eq. (9), on the cavity reduces to the form

$$\begin{aligned} &-\cos\beta^* \iint_S \sigma_c(S^{(Q)})\frac{\partial}{\partial x}\left(\frac{1}{r_{PQ}}\right)\cos\theta^{(Q)}\, ds^{(Q)} \\ &-\sin\beta^* \iint_S \sigma_c(S^{(Q)})\frac{\partial}{\partial R}\left(\frac{1}{r_{PQ}}\right)\cos\theta^{(Q)}\, ds^{(Q)} \\ &+ w_c(x^*)\sin\beta^*\cos\theta^* = 0 \end{aligned} \tag{11}$$

where $w_c(x)$ is given in Eq. (3). Note the boundary condition, Eq. (8), is enforced on the deflected cavity.

Without going into the details of surface integrals in Eqs. (10) and (11), it can be stated that they are integrated over the undeflected body-cavity configuration and are proportional to $\cos\theta^*$ (see Ref. 4). Consequently, it is only necessary to satisfy Eqs. (10) and (11) along one particular meridian, say, along $\theta^* = 0$. The cross flow term w_c involves the cavity deflection $\delta_c(x)$. The integration of these equations by numerical means to obtain the source strength $\sigma_c(S)$ and cavity deflection δ_c is discussed next.

2. Numerical Solution

The numerical solution to be presented here is based on the numerical techniques developed earlier[4] for the cross flow over an axisymmetric rigid body. For the latter case, the only differential equation to be solved is the one given in Eq. (10). For the purposes of numerical integration, the body is divided once again into a finite number, say n, of conical segments. Assuming the source strength on the segment $\sigma_c(S_i)$ is uniform on each segment, the surface integrations are performed on each segment to reduce the integro-differential equation [Eq. (10)] into an algebraic equation. The enforcement of Eq. (10) on each segment then yields n coupled equations in n unknown values of $\sigma_c(S_i)$. The solutions of these linear simultaneous equations yield the desired source strength distribution $\sigma_c(S)$ on the body, which can then be used to determine the velocity potential and flow quantities of interest.

To extend this technique to the problem at hand, one assumes the deflection function $\delta(x)$ of the cavity. This permits the evaluation of the source strength distribution $\sigma_c(S)$ in the manner of a rigid body, provided only one set of equations, either Eq. (10) or Eq. (11), is enforced on the cavity. The satisfaction of the remaining set is used to update the cavity deflection $\delta(x)$. The problem can then be iterated, until all the equations are simultaneously satisfied, to yield the actual deflection $\delta(x)$ and the source strength distribution $\sigma_c(S)$. In the iteration scheme initially developed here, $\sigma_c(S)$ is chosen to satisfy Eq. (11) on the cavity, and the enforcement of boundary condition, Eq. (8), on the cavity is used to update the cavity deflection. For this purpose, one computes the normal velocity $V_{N,c}(x)$ due to the cross flow on the assumed configuration of the deflected cavity and checks whether it is zero or not. A nonzero value suggests that the assumed cavity boundary is not a streamline. Since the actual cavity boundary must be a streamline, its true deflection is such that its tangent vector matches the velocity vector on that portion of the streamline. This leads to the cavity angular deflection increment $\Delta\delta(x)$ required to update the cavity portion:

$$\Delta\delta(x) = \frac{V_{N,c}(S)}{V_T(S)} = \frac{g_c(S) + w_c\cos\beta}{V_T(S)} \tag{12}$$

where $V_T(S)$ is the meridional velocity on the bubble surface due to unit axial flow. The actual bubble angular deflection is then

$$\delta(x)\,|_{\text{new}} = \delta(x)\,|_{\text{old}} + \Delta\delta(x) \tag{13}$$

Having obtained a new cavity configuration, the calculation is repeated and $\delta(x)$ and $\sigma(S)$ are updated. This is repeated until $\Delta\delta(x) \to 0$ on the cavity.

Direct integration of Eqs. (10) and (11) as indicated above leads to a very slow convergence scheme. To improve convergence, it has become necessary not only to satisfy the velocity boundary condition, but also to enforce the appropriate cross flow velocity potential distribution on the cavity surface. To enable such a computational scheme, the velocity potential $\phi_c^*(S)$, with the assumed cavity deflection, is expressed in the form

$$\phi_c^*(S) = \phi_c^*(S_b) - \int_{S_b}^{S} f_c^*(S)\,dS \tag{14}$$

The similar expression with the actual cavity deflection is then

$$\phi_c(S) = \phi_c(S_b) - \int_{S_b}^{S} f_c(S)\,dS \tag{15}$$

Substituting Eq. (9) for $f_c(S)$ and making use of Eq. (14), this can be rewritten as a sum of one known quantity $\bar{\phi}_c(S)$ and another unknown quantity $\delta\phi_c(S)$

$$\phi_c(S) = \bar{\phi}_c(S) + \delta\phi_c(S) \tag{16}$$

where

$$\begin{aligned} \bar{\phi}_c(S) &= \phi_c^*(S) + \int_{S_b}^{S} f_c^*(S)\,dS \\ \delta\phi_c(S) &= \phi_c(S_b) - \phi_c^*(S_b) + \int_{S_b}^{S} w_c \sin\beta\, dS \end{aligned} \tag{17}$$

Note $\phi_c(S_b) - \phi_c^*(S_b)$ is a constant, and approaches zero as the solution converges and $\phi_c^*(S)$ approaches $\phi_c(S)$. Since $w_c(x)$ is a function of cavity deflection angle $\delta(x)$, which is still unknown, $\delta\phi_c(S)$ is also unknown, but finite, and varies along the cavity axis. Now we choose this function such that the boundary condition, Eq. (9), is satisfied. If $\bar{f}_c(S)$ is the tangential velocity associated with $\bar{\phi}_c(S)$ and $\delta f_c(S)$ with that of $\delta\phi_c(S)$, this condition becomes

$$\bar{f}_c(S) + \delta f_c(S) = -w_c \sin\beta \tag{18}$$

In the iteration scheme to be developed here, we recompute $\delta\phi_c(S)$ such that this relation is satisfied. As the solution converges, $\delta f_c(S)$ approaches zero and $\delta\phi_c$ cancels the integral on the right-hand side of the expression for $\bar{\phi}_c(S)$. Then $\phi_c^*(S)$ approaches $\phi_c(S)$. Thus, by this means, one not only satisfies the boundary condition, Eq. (9) on the cavity, but also ensures the tangential velocity function $f_c(S)$ in this relation is derived from the appropriate velocity potential.

Let us now turn to the details of computation of the left-hand side of Eq. (18). To compute the first term, the source strength distribution $\bar{\sigma}_c(S)$ is determined by solving the cross flow problem by satisfying the rigid boundary condition, Eq. (8), on the body and prescribing the velocity potential $\bar{\phi}_c(S)$ on the cavity surface. The tangential velocity $\bar{f}_c(S)$ is then obtained using this source strength distribution. To compute the second term, the cross flow problem is solved to determine $\sigma_c(S;S^*)$ by enforcing zero normal velocity, [Eq. (8)] on the missile surface, and unit value of the velocity potential at station x^*, that is, $\delta(S-S^*)$ on the cavity. If $f_c(S;S^*)$ is the derivative of the resulting velocity potential, one has by superposition

$$\delta f_c(S) = \int_{\text{cavity}} f_c(S;S^*)\delta\phi_c(S^*)\,dS^* \tag{19}$$

where $\delta\phi_c(S)$ is still unknown. The imposition of Eq. (18) at a finite number of points along the cavity yields a linear set of coupled simultaneous equations, which are then solved for these unknowns. Knowing this distribution, the net source strength distribution on the body-cavity surface is calculated

$$\sigma_c(S) = \bar{\sigma}_c(S) + \int_{\text{cavity}} \sigma_c(S;S^*)\delta\phi_c(S^*)\,dS^* \tag{20}$$

Having obtained the source strength, one can compute the velocity potential $\phi_c(S)$ and the velocity component $V_{Nc}(S)$ normal to the cavity surface. The use of this relation in Eq. (12) determines the function $\Delta\delta(x)$, and hence the corrected cavity deflection function. The problem is now iterated until the solution for the cavity deflection $\delta(x)$ has converged.

B. Cross Flow Solution with Angular Rotation (Nonuniform Cross Flow)

Consider now the case of axisymmetric body with an attached cavity of known geometry moving axially with unit velocity, and rotating slowly about its center of gravity in the x-z plane. As long as the angular rotation is such that the angle of attack remains small all along the body-cavity length, the simplification of Appendix B is applicable. The cross flow velocity on the body-cavity system acting in the z-direction is given by

$$\begin{aligned} w_c(x) &= qx && -l_B \le x \le l_n \\ &= qx - \delta(x) && x < -l_B \end{aligned} \tag{21}$$

where $\delta(x)$ is the angular deflection of the cavity about the body axis. Note this is different from the case treated in the earlier section in that the cross flow is not constant, but varies linearly with x along the body.

The computation of cross flow perturbation potential ϕ_c corresponding to rotational velocity, $q \ll 1$, proceeds the same way as described in the earlier section. In fact, it is exactly the same except w_c is now replaced with Eq. (21) and an additional term, $-qR(x^*)\sin\beta^*\cos\theta^*$ is included on the left-hand side of Eq. (10). This term arises from resolving the rotation-induced axial component of velocity on the body surface in the direction normal to the body.

III. Computation of Pressure and Hydrodynamic Coefficients

In the numerical computation of pressure and hydrodynamic force coefficients using Eqs. (A7) and (A10), respectively, of Appendix A, the perturbation quantities ϕ_w, f_w associated with unit motion of the body in the z-direction and ϕ_q, f_q associated with unit rotation of the body about its center of gravity in the x-z plane are required. The cross flow solutions ϕ_c, f_c obtained in Secs. II.A and II.B correspond respectively to uniform motion of the body with velocity α_B in the z-direction, and rotational velocity q, which is much less than unity. To obtain the desired quantities, these solutions are scaled up by dividing the cross flow solution obtained in Sec. II.A with α_B and those of Sec. II.B with q values used in those computations. Note that such a procedure is valid as long as the angles of attack experienced by the body-cavity system during planar motion remain small. Obviously, the results so computed are not accurate for large body translations and rotations.

Note that the pressure distribution and hydrodynamic coefficients are computed using the relations derived for the rigid body in planar motion, but the unit perturbation potentials, and their derivatives appearing therein, are computed taking cavity deflection into account.

In Secs. II.A and II.B the boundary condition, Eq. (9), enforced on the cavity implies that the normal force acting on it is zero. This usually means the perturbation potential ϕ_c is not identically zero on the cavity. Thus, the hydrodynamic inertia coefficients $C_{N\dot{\alpha}}$ and $C_{N\dot{q}}$ turn out to be nonzero on the cavity. In reality, these should be identically zero since the cavity cannot sustain any normal force due to normal ac-

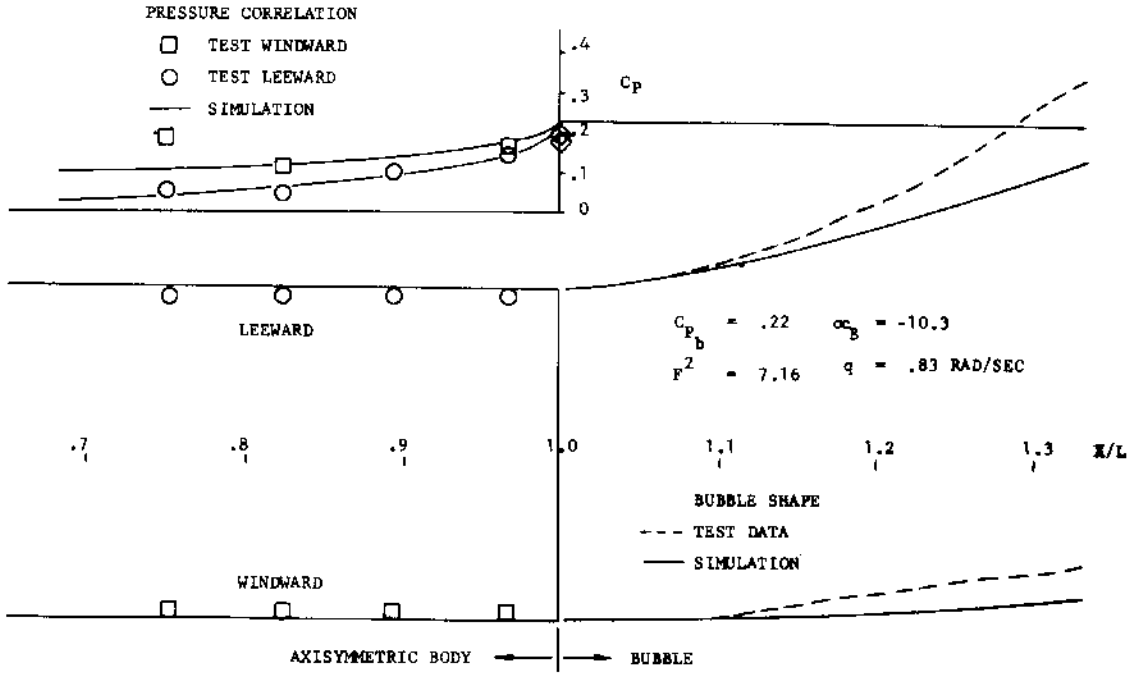

Fig. 2 Comparison of computed pressure distribution and bubble deformation with test data.

celeration either. In other words the cavity bends during acceleration normal to the body axis. To determine the inertia coefficients more accurately within the framework of the present formulation, the cross flow potentials ϕ_c in Secs. II.A and II.B are solved again by replacing Eq. (9) with $\phi_c = 0$ on the cavity. The numerical scheme is appropriately modified to reflect this change though for the sake of brevity it is not discussed here. The inertia coefficients presented in the following section are the values so computed.

IV. Numerical Results

For the purpose of validating the solution developed here for the mixed boundary value problem in potential flow, the computations of pressure distributions on typical axisymmetric bodies are made and compared with the measured data from scale model tests. These tests were conducted in the Lockheed Underwater Missile Test Facility, and consisted of launching scale model missiles vertically upward from a submerged platform using air as a launch gas. Since the asymmetric cavity deflection predominately affects the pressure field on the rear cylindrical portion of the missile, pressure data was acquired on the missile near its base, and along the windward and leeward meridians. As the missile kinematics change along the trajectory, the pressure on the missile at a given location also changes with time. For comparison, the pressure was thus chosen at one particular instance, and the missile kinematics at that instance used in computing the pressure field on the missile. The appropriate expression used for this purpose is given in Eq. (A7) of Appendix A.

Figure 2 presents the measured pressure coefficient C_p ($=p/\frac{1}{2}\rho U^2$) along the two meridian lines compared with the computed results. The particular kinematics of the missile at the instance of comparison are identified in this figure. Translational and rotational accelerations are present, but their contributions to the pressure distribution are found to be minimal and ignored here. Note, as one would expect the theoretical pressure distribution in the bubble ($x/L > 1.0$, x is measured from the nose) remains constant. On the missile, the computed results agree well with measured data except for one transducer location on the windward side. The pressures on both leeward and windward meridians approach the base pressure and become identical at the base.

Also presented in Fig. 2 are the tail bubble deformations at the instant the pressure comparison was made. The analytical deformation of the bubble was determined by computing the deformations associated with lateral and rotational motions of the missile separately and adding them. The acceleration effects are once again ignored. The measured bubble configuration is obtained from the optical data acquired by photographing the missile as it passes through fixed elevations. The agreement is reasonably good near the base, but differences between the test and computation increase with distance from the missile base. This is understandable in that the analytical model's validity degrades as the solution progresses away from the base, since the mixed boundary conditions are enforced only in the neighborhood of the base and not on the entire cavity. The main purpose of this paper is to present a method to compute the pressures and forces on the missile taking into account the asymmetric cavity deformation. The fact that the computed pressure field on the missile agrees well with measurements in the neighborhood of the base provides the justification for the approximation made in the analytical simulation.

The normal force acting on the missile is proportional to the pressure difference across the missile in the direction normal to the axis. The excess pressure along the windward meridian over that along the leeward meridian is shown in nondimensional form in Fig. 3 for different flight conditions. The symbols indicate the data points obtained from tests and the solid-line data obtained from solving the mixed boundary value problem described in this paper. The agreement seems to be reasonably good, especially at small angles of attack, where the theory should be most accurate.

The two parameters that influence the cavity shape are the Froude number and the base pressure coefficient (or the cavitation number). To evaluate how these parameters influence the actual hydrodynamic forces acting on the missile, the hydrodynamic coefficients were computed for a typical axisymmetric missile over a range of Froude number F and base pressure coefficient C_{p_b} of practical interest. For the sake of ease in presentation, each coefficient has been normalized with respect to its value at $C_{p_b} = 0$ and $F^2 = 5$. The static force and moment coefficients so obtained are shown in Fig. 4, first varying Froude number, and keeping base pressure coefficient constant; and second, varying base pressure coefficient, and keeping Froude number constant. As the curves would indicate, the effect of Froude number on hydrodynamic coefficients is less than 1%, and is much smaller than that of the base pressure coefficient. The variation in coefficients appears to be larger with decrease of the base pressure

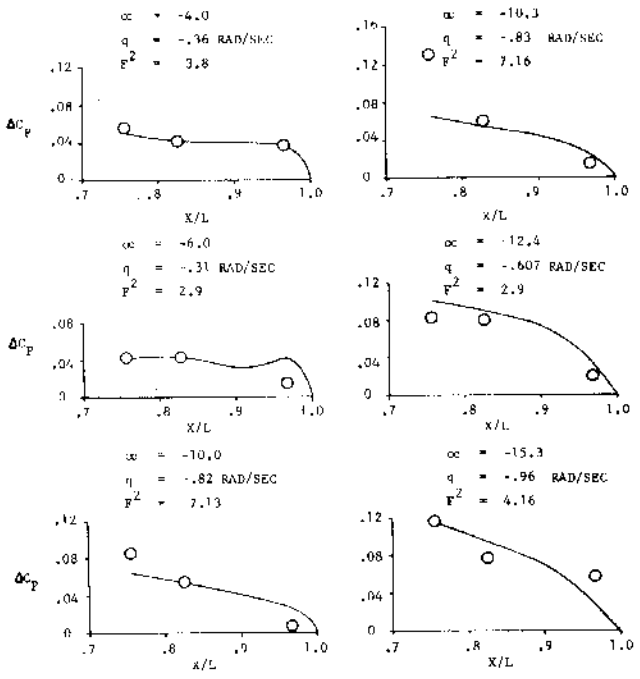

Fig. 3 Comparison of computed pressure difference across the missile with measurement.

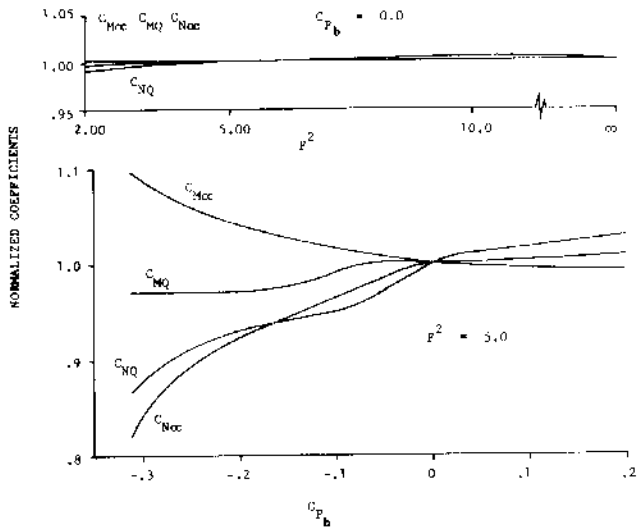

Fig. 4 Variation of hydrodynamic coefficients (static) with Froude number and base pressure coefficient on a typical axisymmetric body.

coefficient. These results suggest that if base pressure fluctuations are large along the projectile path, the hydrodynamic coefficients need to be adjusted accordingly for accurate prediction of its trajectory.

The potential flow, mixed boundary value problem, as suggested here for axisymmetric bodies with trailing cavities, is very complex and involves much effort and computer cost. In the past, one way of computing hydrodynamic coefficients of missiles with asymmetric cavities was to approximate the trailing cavity as a rigid extension of the missile body. Since this required only a single hard boundary solution of the Neumann program, the problem was considerably simplified. To indicate the essential differences between such an approximation and the exact solution as obtained in this paper, the comparisons of pressure and force coefficient distributions are presented in Figs. 5-7. In these calculations, the cavity is

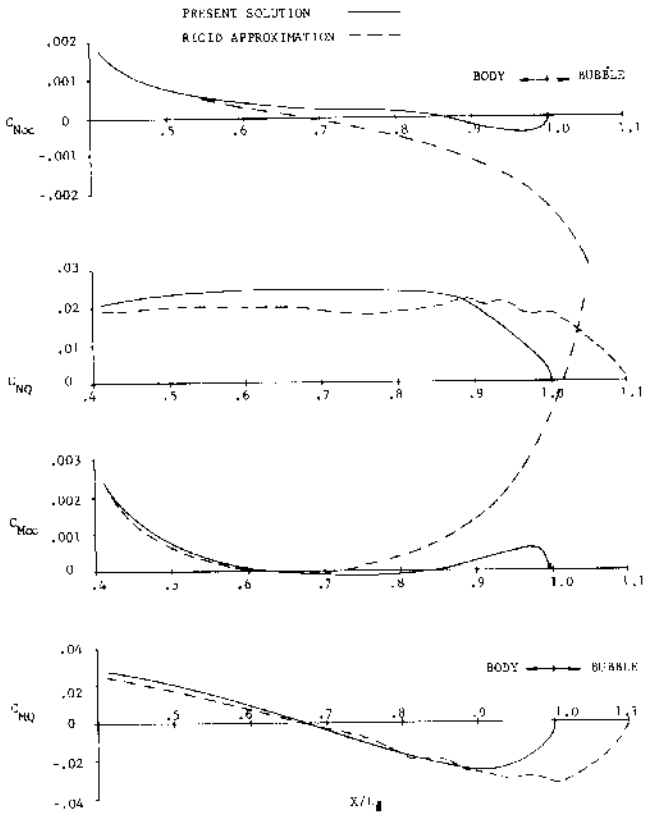

Fig. 6 Comparison of static hydrodynamic coefficients with different representation for the trailing cavity.

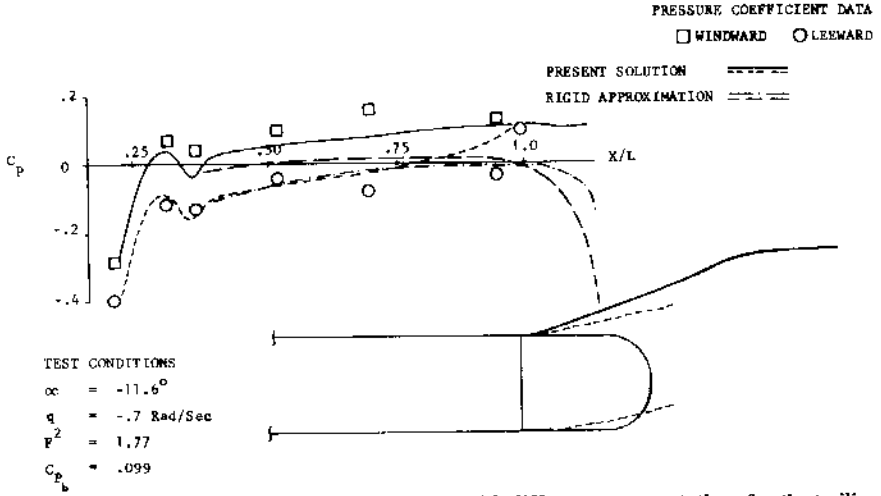

Fig. 5 Comparison of computed pressure distribution with different representations for the trailing cavity.

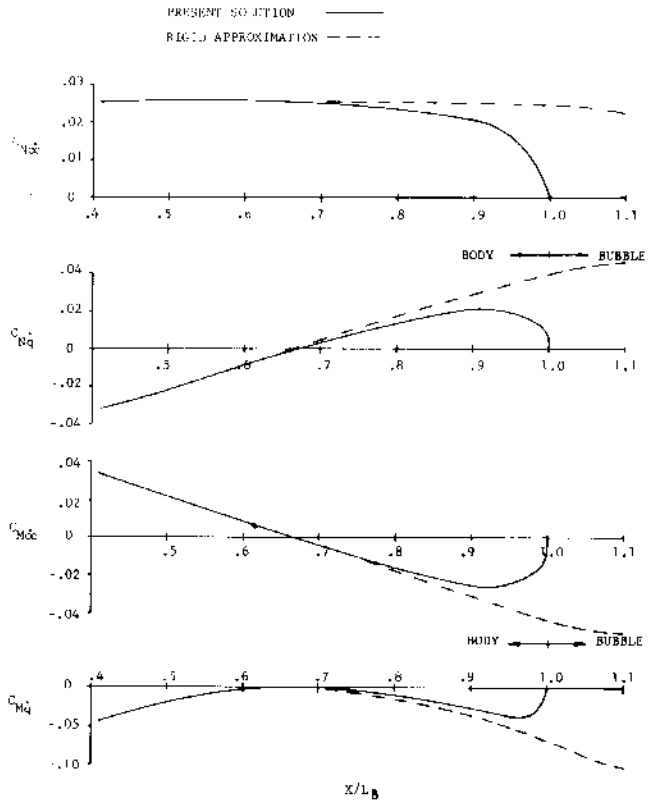

Fig. 7 Comparison of inertia coefficients with different representations of the trailing cavity.

represented by a straight cylindrical extension of the missile one-quarter of its length with a hemispherical closure at its end. Note the pressure distributions along the windward and leeward meridians are very close in the rigid cavity case and become zero at the base of the missile. In actual cases, the base pressure coefficient need not be zero. For the particular test case shown in Fig. 5, the base pressure coefficient is equal to 0.099 and the present solution approaches that value on both meridians near the base. Away from the base, the approximate solution matches the exact one along the leeward but not on the windward meridian. This must be the result of the deflection of the cavity, which is included in the exact solution. At any rate, the pressure difference across the missile is larger in the exact solution than in the approximate case. This is in general agreement with the measured data.

Figure 6 presents the hydrodynamic force and moment coefficient distributions on a typical axisymmetric body as computed by these two methods. Since the bubble cannot resist any force, these coefficients should assume zero values at the base. This is evident in the exact solution but not in the approximate case. The integrations of these distributions over the length of the missile differ somewhat, the difference for certain coefficients reaching as much as 10%.

Figure 7 compares the hydrodynamic inertia coefficients computed by the two methods. Note that, once again, the present solution yields results that are physically meaningful near the base, while the approximate solution does not.

V. Conclusions

An iterative computational scheme has been developed to calculate the potential flow solution of an axisymmetric body with trailing cavity when in planar motion. As long as the motion in the axial direction is predominant, the cavity configuration (cross-sectional radius) is assumed to be governed by this axial motion alone. The effect of lateral translation and rotation of the body in planar motion is to deflect the cavity in its plane of motion. Assuming that lateral translation and body rotation are small, solutions are constructed separately by imposing the mixed boundary conditions, namely zero normal velocity on the body, and zero normal force on the deflected cavity. Initially, the cavity deflection is unknown, but is computed iteratively by adjusting its deflection until the normal velocity on its surface is zero. The solutions obtained for a body's lateral motion and rotation are then combined with that of the axial motion to obtain the resultant planar motion of the body-cavity system.

In the presence of lateral motion and/or body rotation, the body-cavity configuration is essentially nonaxisymmetric. For small lateral disturbances, the problem is simplified to one of an axisymmetric case with surface source strength modified to account for cavity deflection. The analytical technique presented here thus represents an approximate way of solving the body-cavity problem in planar motion and is valid for small cavity deflection angles.

As a means of validation, pressure distributions computed for an axisymmetric missile in planar flight were compared with measurements made during vertical launches of the model missile under Froude and cavitation scaled conditions. In the region of the missile base differences in pressure across the windward to leeward body surface, as predicted from the theory, compared quite satisfactorily with observed pressure test data, and provided justification for the analytical methods presented herein.

The underwater performance of the missile is normally measured with its hydrodynamic coefficients. The sensitivity study of these coefficients, with Froude number and base pressure coefficient, has indicated that the effect of the former is relatively negligible to that of the latter. This suggests that in trajectory computations the hydrodynamic coefficients need be represented as functions of base pressure coefficient if base pressure fluctuations are expected to be large.

In the past, missile hydrodynamic coefficients have been evaluated by treating the cavity as a rigid cylindrical extension of the missile itself. Such a solution is independent of cavitation number (base pressure coefficient) and Froude number but dependent on the cavity length. For lack of other means, the cavity length was selected to match the measured trajectories in simulated scale model tests. The essential differences between this approximate model and the exact method developed here have been pointed out by comparing the pressure and coefficient distributions on the missile as predicted by these methods.

Appendix A: Force and Moment Relations for a Body in Planar Motion

An axisymmetric body with a trailing cavity is in planar motion in an infinite fluid medium. Unless the motion is purely axial, the cavity deflects in the plane of motion. As long as such deflection is small, let us assume for now that the flowfield around this asymmetric body-cavity configuration can be calculated by performing computations on the undeformed configuration with source strength, however, accounting for the deflection. Now, let the x, y, z coordinate system be attached to this, with origin located at 0, the mass center of the body, on the axis of symmetry. Let us assume the body is moving, say, with velocity components u and w along x and z axis, and rotational velocity q about y axis (see Fig. 1 for sign convention). The velocity components of this motion at a point P on the body in normal, tangential, and circumferential directions, respectively, are

$$V_N = -u\sin\beta + w\cos\beta\cos\theta - q(R\sin\beta + x\cos\beta)\cos\theta$$

$$V_S = u\cos\beta + w\sin\beta\cos\theta + q(R\cos\beta - x\sin\beta)\cos\theta \qquad \text{(A1)}$$

$$V_\theta = -(w - qx)\sin\theta$$

where β is related to the body slope at P and is given by

$$dR/dx = \tan\beta \qquad \text{(A2)}$$

Here $R(x)$ represents the body radius. The disturbance velocity potential, ϕ, of fluid flow associated with the body motion can be expressed in the form

$$\phi(x,r,\theta) = u\phi_u(x,r) + w\phi_w(x,r)\cos\theta + q\phi_q(x,r)\cos\theta \quad \text{(A3)}$$

where $\phi_u(x,r)$, $\phi_w(x,r)$, and $\phi_q(x,r)$ are the unit velocity potentials associated with unit axial, normal, and pitch motions respectively in the meridional plane $\theta = 0$. Using the convention of negative gradient of this potential as the fluid velocity, one can obtain the three fluid velocity components at point P on the body, in normal, tangential, and circumferential directions.

$$-\frac{\partial\phi}{\partial N} = ug_u(x,R) + [wg_w(x,R) + qg_q(x,R)]\cos\theta$$

$$-\frac{\partial\phi}{\partial S} = uf_u(x,R) + [wf_w(x,R) + qf_q(x,R)]\cos\theta \quad \text{(A4)}$$

$$-\frac{\partial\phi}{R\partial\theta} = (1/R)[w\phi_w(x,R) + q\phi_q(x,R)]\sin\theta$$

Here $g_u(x,R), \ldots f_q(x,R)$ are related to velocity potential derivatives in normal and tangential directions.

$$g_i = -\frac{\partial\phi_i}{\partial N} = \left\{-\frac{\partial\phi_i}{\partial x}\sin\beta + \frac{\partial\phi_i}{\partial r}\cos\beta\right\}_{r=R} \quad (i = u,w,q) \quad \text{(A5)}$$

$$f_i = -\frac{\partial\phi_i}{\partial S} = -\left\{\frac{\partial\phi_i}{\partial x}\cos\beta + \frac{\partial\phi_i}{\partial r}\sin\beta\right\}_{r=R}$$

The relative velocity of fluid with respect to the body is then obtained by subtracting the body velocity, Eq. (A1), from the fluid velocity, Eq. (A4). The resulting relative velocity components are

$$q_N = u(g_u + \sin\beta) + [w(g_w - \cos\beta) + q(g_q + R\sin\beta + x\cos\beta)]\cos\theta$$

$$q_S = u(f_u - \cos\beta) + [w(f_w - \sin\beta) + q(f_q - R\cos\beta + x\sin\beta)]\cos\theta$$

$$q_\theta = \{w(1 + \phi_w/R) + q(\phi_q/R - x)\}\sin\theta \quad \text{(A6)}$$

In solving for the velocity potential, the boundary condition, $q_N \equiv 0$, will be enforced; consequently q_S and q_θ are the only two nonzero velocity components on the body surface. Using the unsteady Bernoulli equation, the pressure field on the moving body can be expressed as

$$p(x,R,\theta) = \rho[\dot{u}\phi_u + \dot{w}\phi_w\cos\theta + \dot{q}\phi_q\cos\theta + \tfrac{1}{2}(V_N^2 + V_S^2 + V_\theta^2 - q_S^2 - q_\theta^2) + g(x + l_b)] \quad \text{(A7)}$$

In this relation, the dot over a quantity represents the time derivative of that quantity; g represents the gravitational potential acting in the negative direction of the x-axis, and, for convenience, the gravity level is referenced at the base of the body. The axial force F_x, normal force F_z, and pitching moment M_y resulting from this pressure distribution are

$$F_x = \iint_{S_B} pR\tan\beta\,d\theta\,dx \qquad F_z = -\iint_{S_B} pR\cos\theta\,d\theta\,dx$$

$$M_y = \iint_{S_B} pR(x + R\tan\beta)\cos\theta\,d\theta\,dx \quad \text{(A8)}$$

Here surface integral extends over the surface of the body. Substituting relations, Eqs. (A1) and (A6) in the pressure relation, Eq. (A7) and the resulting expression in Eq. (A8), yields after the θ-integration and neglecting the terms involving squares and products of w and q

$$F_x = \tfrac{1}{2}\rho A_b[C_{x\dot{u}}\dot{u}d - C_{xuu}u^2]$$

$$F_z = -\tfrac{1}{2}\rho A_b[C_{N\dot{\alpha}}\dot{w}d + C_{N\dot{q}}\dot{q}d^2 + C_{N\alpha}wu + C_{Nq}uqd]$$

$$M_y = \tfrac{1}{2}\rho A_b d[C_{M\dot{\alpha}}\dot{w}d + C_{M\dot{q}}d^2 + C_{M\alpha}wu + C_{Mq}uqd] \quad \text{(A9)}$$

where

$$C_{xu} = \frac{4\pi}{A_b d}\int_{-l_B}^{l_n}\phi_u R\tan\beta\,dx$$

$$C_{xuu} = -\frac{2\pi}{A_b}\int_{-l_B}^{l_n} R\tan\beta[1 - (f_u - \cos\beta)^2]\,dx$$

$$C_{N\dot{\alpha}} = \frac{2\pi}{A_b d}\int_{-l_B}^{l_n}\phi_w R\,dx$$

$$C_{N\dot{q}} = \frac{2\pi}{A_b d^2}\int_{-l_B}^{l_n}\phi_q R\,dx$$

$$C_{N\alpha} = \frac{2\pi}{A_b}\int_{-l_B}^{l_n} R(\cos\beta - f_u)(f_w - \sin\beta)\,dx$$

$$C_{Nq} = \frac{2\pi}{A_b d}\int_{-l_B}^{l_n} R[R + (\cos\beta - f_u)(f_q - R\cos\beta + x\sin\beta)]\,dx$$

$$C_{M\dot{\alpha}} = \frac{2\pi}{A_b d^2}\int_{-l_B}^{l_n} R(x + R\tan\beta)\phi_w\,dx$$

$$C_{M\dot{q}} = \frac{2\pi}{A_b d^3}\int_{-l_B}^{l_n} R(x + R\tan\beta)\phi_q\,dx$$

$$C_{M\alpha} = \frac{2\pi}{A_b d}\int_{-l_B}^{l_n} R(\cos\beta - f_u)(f_w - \sin\beta)(x + R\tan\beta)\,dx$$

$$C_{Mq} = \frac{2\pi}{A_b d^2}\int_{-l_B}^{l_n} R[R + (\cos\beta - f_u)(f_q - R\cos\beta + x\sin\beta)] \times (x + R\tan\beta)\,dx \quad \text{(A10)}$$

In these relations, A_b refers to reference area (usually base area), and d to reference diameter (usually base diameter). The integration in the above relations extends over the length of the body. Once the calculation of unit potentials ϕ_u, ϕ_w, and ϕ_q, and the velocities f_u, f_w, and f_q are accomplished, the hydrodynamic coefficients $C_{x\dot{u}}$, C_{xuu}, $C_{N\dot{\alpha}}$, $C_{N\dot{q}}$, $C_{N\alpha}$, C_{Nq}, $C_{M\dot{\alpha}}$, $C_{M\dot{q}}$, $C_{M\alpha}$, and C_{Mq} can be calculated from the above integral relations.

The above relations are also equally applicable for the cavity surface. In the presence of either lateral translation or pitch motion, the cavity deflects to the new configuration where no normal force exists. Consequently, on the cavity

$$\frac{\partial C_{N\dot{\alpha}}}{\partial x} = \frac{\partial C_{N\dot{q}}}{\partial x} = \frac{\partial C_{N\alpha}}{\partial x} = \frac{\partial C_{Nq}}{\partial x} = 0 \quad \text{(A11)}$$

These conditions will be used in evaluating the cavity deflection.

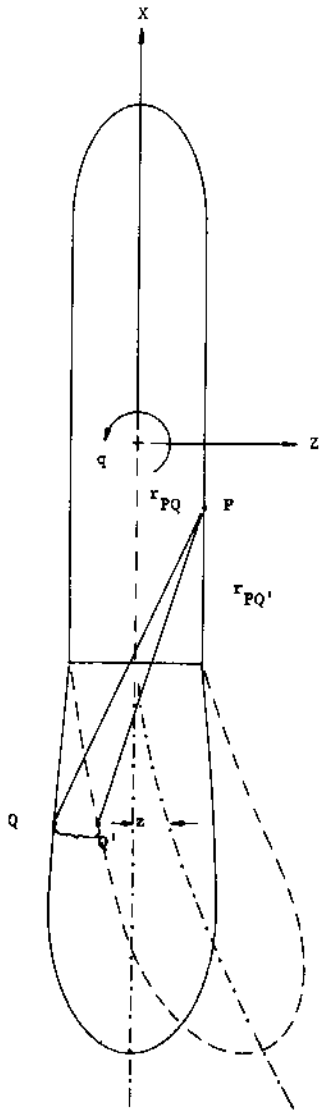

Fig. B1 Sketch illustrating the approximation.

Appendix B: Basis of Problem Simplification

Consider a rigid body in motion with trailing cavity slightly deflected as shown in Fig. B1. Let Q and Q' be the positions of the same point on the cavity surface before and after deflection. The cross flow potential, $\phi_c^{(P)}$ at the point, $P(x^*,R^*,\theta^*)$ on the body-bent cavity system can be expressed by the surface integral of the source strength at the variable point $Q'(x',R',\theta')$ times the reciprocal distance between points P and Q':

$$\phi_c^{(P)} = \iint_S \frac{\sigma_c(S')\cos\theta'}{r_{PQ'}}\,ds' \tag{B1}$$

Here $\sigma_c(S')\cos\theta'$ represents the source strength at point Q' and the surface integral extends over the whole body-cavity surface. Note the source strength depends on the cavity deflection; however, as long as the deflection angle is small, it is assumed that its dependence on the circumferential angle θ still remains the same as on an undeflected cavity, while its magnitude changes somewhat. Also, it is assumed the cross sections of the cavity remain circular after deflection. If $Z_c(x)$ represents the cavity deflection in the x-z plane, the above integral can be expanded in the form

$$\phi_c^{(P)} \simeq \iint_S \frac{\sigma_c(S')\cos\theta'}{r_{PQ}} \times \left\{1 - \frac{[Z_c(x^*) - Z_c(x')]\,[R^*\cos\theta^* - R'\cos\theta']}{r_{PQ}^2}\right\} ds' \tag{B2}$$

Note that for points P and Q on the rigid body, $Z_c(x^*) \equiv 0$ and $Z_c(x) \equiv 0$, and hence only the first integral remains. For other cases, the second term contributes, but its contribution is smaller the farther the points P and Q are. As the points come closer, $Z_c(x^*) - Z_c(x')$ decreases, and for points on the same cross section it is identically zero. Conveniently, the second term can be neglected, at least to a first approximation. Thus, the potential for the body-bent cavity system reduces to the integral

$$\phi_c^{(P)} \simeq \iint_S \frac{\sigma_c(S')\cos\theta'}{r_{PQ}}\,ds' \tag{B3}$$

where the surface integral is restricted to the axisymmetric undeformed configuration. Note however, the source strength variation $\sigma_c(S')$ along the axis is different from that of the undeformed configuration. The variation in $\sigma_c(S)$ is such that it accounts for the appropriate modification of the flowfield associated with deflected cavity.

Acknowledgments

This work was supported in part by Missile Systems Division of Lockheed Missiles & Space Company, Inc. under its Independent Development Program.

References

[1] Nelson, D.M., "Hydrodynamic Coefficient Calculation Using Douglas Potential Flow Computer Program," NAVWEPS Report 8799, NOTS TP 3905, U.S. Naval Ordnance Test Station, China Lake, Calif., Oct. 1959.

[2] Struck, H.G., "Discontinuous Flows and Free Streamline Solutions For Axisymmetric Bodies at Zero and Small Angles of Attack," NASA TN D-5634, Feb. 1970.

[3] Rattayya, J.V., Brosseau, J.A., and Chisholm, M.A., "Potential Flow about Bodies of Revolution with Mixed Boundary Conditions—Axial Flow," *Journal of Hydronautics*, Vol. 15, Jan. 1981, pp. 74-80 (this issue).

[4] Hess, J.L., "Calculation of Potential Flow About Bodies of Revolution Having Axes Perpendicular to the Free Stream Direction," Douglas Aircraft Company Report No. ES29812, Oct. 1960.